Noninvasive Identification of Three-dimensional Myocardial Infarctions from Inversely Reconstructed Equivalent Current Density

Zhaoye Zhou[1], Chengzong Han[1], Bin He[1,2]

[1]Department of Biomedical Engineering, University of Minnesota, Minneapolis, USA
[2]Institute for Engineering in Medicine, University of Minnesota, Minneapolis, USA

Abstract

The study presents a new approach to non-invasively identify the 3-dimensional MI substrate from the equivalent current densities (ECDs) that is inversely reconstructed from body surface potential maps (BSPMs). The MI substrate was characterized using a threshold determined from the ECD magnitude. A total of 114 sites of transmural infarctions, 91 sites of epicardial infarctions, and 36 sites of endocardial infarctions were simulated. The results show that: 1)With 205 BSPM electrodes and 10 μV Gaussian white noise, the averaged accuracies for transmural MI are sensitivity = 83.4%, specificity = 82.2%, and the distance between the centers of gravity (DCG) = 6.5mm. Epicardial infarctions (sensitivity = 81.6%, specificity = 75.8%, and DCG = 7.5mm) obtained similar accuracies to endocardial infarctions (sensitivity = 80.0%, specificity = 77.0%, and DCG = 10.4 mm). A reasonably good imaging performance was obtained under a higher noise level, fewer BSPM electrodes, and mild volume conductor modeling error, respectively. The results suggest that this method is capable of imaging the transmural and surface infarction.

1. Introduction

Myocardial infarction (MI) is caused by the occlusion of coronary arteries leading to the formation of electrophysiologically-abnormal substrate, and is responsible for initiating lethal ventricular arrhythmias [1]. The noninvasive identification of MI substrate based on the electrophysiological alternation is crucial for the clinical management of cardiac arrhythmias. In the past decades, many efforts have been made in this aspect to develop the cardiac electrical source imaging techniques, which reconstruct the cardiac electrical properties by solving the ECG inverse problem. Considering the 3-D volume of the heart, this technique has been extended from 2-D [2], [3] to 3-D [4]-[7], including a physical-model-based 3-dimensional cardiac electrical imaging (3DCEI) approach which reconstructs the equivalent current density (ECD) distribution. This method has been proven to be promising on visualizing 3-dimensional (3-D) cardiac activation sequence in both computer simulation and animal experiment [6]-[7].

In the present study, we have extended the above-mentioned technique into imaging the MI substrate in the pathological heart. A total of 114 sites of transmural MI and 127 sites of surface MI were simulated to evaluate the proposed method. The body surface potential maps (BSPMs) with MI were simulated by means of a cellular automaton heart model embedded in a piece-wise homogeneous heart-torso volume conductor. The MI substrates were inversely estimated from the BSPMs and the results were compared with simulated "true" MI substrate to assess the performance of the proposed method.

2. Method

2.1. Principles of imaging MI from ECD distribution

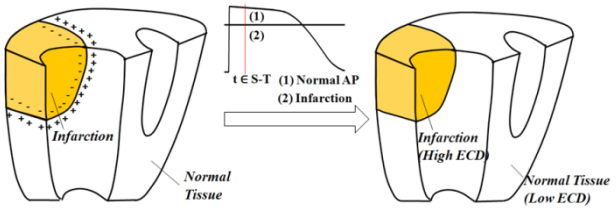

Figure 1. The principle of imaging MI from ECD.

In MI, the blockage of coronary blood supply creates substrates with altered electrophysiological properties, resulting in the central necrosis tissue which is usually considered electrically unexcitable [1]. During S-T segment, the transmembrane potential (TMP) of normal myocardial cells rises to the plateau potential while the TMP of infarcted ones remains unchanged, resulting in a voltage gradient surrounding the MI border (figure 1). This important feature of the TMP spatial gradient during

S-T segment provides an alternative and equally effective way to characterize the MI substrates. As the local equivalent current density (ECD) at each myocardial site is defined to be proportional to the TMP spatial gradient [8], the MI substrates could thus be identified from the ECD distribution during the S-T segment.

The relationship between the ECD distribution and the measurable body surface potentials can be described by the following linear equation:

$$\Phi(t) = LJ(t) \quad (1)$$

Where $\Phi(t)$ is an $M \times 1$ column vector of body surface potentials from M body surface electrodes at time t, $J(t)$ is a $3N \times 1$ column vector of ECD distribution from N myocardial grid points, and L is the $M \times 3N$ transfer matrix that relates the ECD distribution to the body surface measurements. This linear inverse problem was solved using the weighted minimum norm (WMN) estimation [6], [9], [10], which minimizes the following objective function:

$$\min_{J(t)} (\| \Phi(t) - LJ(t) \|_2^2 + \lambda \| WJ(t) \|_2^2 \quad (2)$$

Where W is the Kronecker product of a 3×3 identity matrix I and a $N \times N$ diagonal matrix Ω. λ is the regularization parameter, which can be determined by the L-curve method [11]. Therefore the ECD distribution at time t can be estimated as $J_{est}(t)$. It is noted that the solution of the linear inverse problem leads to a smoothed distribution of ECD. Hereby, the MI substrate and its' border would have an ECD magnitude higher than a predefined value in the S-T segment. It could therefore be identified by defining a threshold that is equal to the certain percentage of the spatial ECD maximum magnitude, expressed as:

$$Threshold = \partial * \arg\max(J_{ave}) \quad (3)$$

where ∂ is the predefined threshold and J_{ave} is the temporal average of 30 ms of the $J_{est}(t)$ inversely estimated from S-T BSPM. Myocardial tissue with a J_{ave} that is higher than the threshold is identified as the substrate of infarction.

2.2. Computer simulation

To evaluate the performance of the method, computer simulations were performed using a cellular automaton heart model with a spatial resolution of 1.5mm and pre-defined electrical properties for myocardial tissues. The cellular automaton heart is embedded in a realistic-geometric piece wise homogeneous heart-torso volume conductor model [4], [5]. The LV myocardium was divided into 17 segment based on the American Heart Association (AHA) standard [12]. The body surface potential maps (BSPMs) were generated from forward computation. The ECD was then reconstructed from BSPM during S-T segment with a time window of 30ms and averaged over time. The MI substrate was then defined, based on the predefined threshold.

We've simulated 114 sites of transmural MI substrates, 91 epicardial infarctions, and 36 endocardial infarctions, with different sizes and various locations throughout the entire LV. Single or a combination of multiple adjacent segments were selected as the MI substrate with altered electrophysiological properties. The simulated transmural infarctions ranged from 5.1% to 38.2% of the LV volume. The surface infarctions have a thickness of approximately 1/3 - 1/2 of the transmural ones. The sizes of the epicardial infarctions varied from 5.6% to 22.9% of the LV volume, while the sizes of the endocardial infarctions varied from 4.4% to 14.9% of the LV volume.

To investigate the effect of noise level, the forward calculated BSPMs were contaminated by Gaussian white noise (GWN) with different noise levels of 0 μV, 5 μV, 10 μV, 15 μV, 20 μV, and 30 μV. Meanwhile, we used different numbers of ECG surface electrodes (256, 205, 182, 156, and 98) to examine the effect of electrode density on the proposed method with additive 10μV level GWN. The effect of volume conductor modeling errors was also studied by adding 10% torso geometry uncertainty and 4mm heart position uncertainty.

2.3. Statistical analysis

Three parameters were computed to quantify the performance: sensitivity, specificity and distance between the centers of gravities (DCG). They are defined as follows:

$$\text{Sensitivity} = TP/(TP+FN) \quad (5)$$

$$\text{Specificity} = TN/(TN+FP) \quad (6)$$

Where true positive (TP) is the volume of true infarction that is correctly identified, false negative (FN) is the volume of true infarction that is mistakenly considered as normal tissue, true negative (TN) is the volume of true normal tissue that is correctly identified as normal, and false positive (FP) is the volume of normal tissue that is mistakenly characterized as infarction. Sensitivity represents the percentage of the accurately estimated infarction in the true infarction, and specificity represents the percentage of the accurately estimated normal region in the true normal tissue. DCG is defined as the Euclidean distance between the gravity center of the estimated infarction and that of the true infarction.

3. Results

3.1. Transmural infarctions

Figure 2 depicts examples of imaging the transmural MI substrates that were located at the anterior, posterior, lateral, and septal of LV. The simulations were performed with 205 surface electrodes and 10-μV additive GWN. The normal tissue, simulated true infarction, and the overlap between simulated infarction and imaged infarction are shown in transparent gray, solid red and solid yellow, respectively. The imaged MI substrates were in good consistency with the simulated MI substrates. The overall performance was evaluated from 114 simulated transmural MI substrates, and on average, sensitivity was 83.4% ± 16.7%, specificity was 82.2% ± 12.9%, and DCG was 6.5 ± 3.5 mm, based on a 50% threshold.

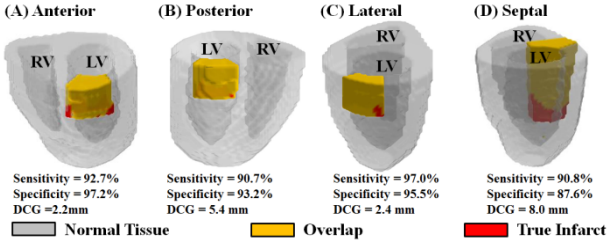

Figure 2. Results for transmural infarction. LV = left ventricle; RV = right ventricle.

3.2. Epicardial and endocardial infarctions

Figure 3 gives representative examples of imaging epicardial infarctions located at anterolateral LV (figure 3(A)) and endocardial infarction located also at anterolateral LV (figure 3(B)). Their positions on the myocardium (epicardium vs. endocardium) were also successfully identified by localizing the spatially maximal ECD (figure 3, black asterisks). The average accuracies of 91 epicardial infarctions are 81.6% ± 15.4% for sensitivity, 75.8% ± 15% for specificity, and 7.5 ± 2.8 mm for DCG. Sixty-five out of 91 epicardial infarctions have been successfully recognized to be epicardial as the corresponding maximal ECD magnitude locates at the LV epicardium. The endocardial infarctions were imaged with an averaged sensitivity of 80.0% ± 15.1%, specificity of 77.0% ± 9.5%, and DCG of 10.4 ± 2.9 mm. A total of 22 out of the 36 cases have been successfully identified as endocardial infarctions. Compared with endocardial infarcts, the epicardial infarcts were estimated with smaller localization error (DCG: 7.5mm vs. 10.4 mm) and slightly higher accuracies (sensitivity: 81.6% vs. 80.0 %). Moreover, non-transmural infarctions are more challenging than the myocardial infarctions, which are reflected by generally higher averaged sensitivity and specificity, and lower DCG.

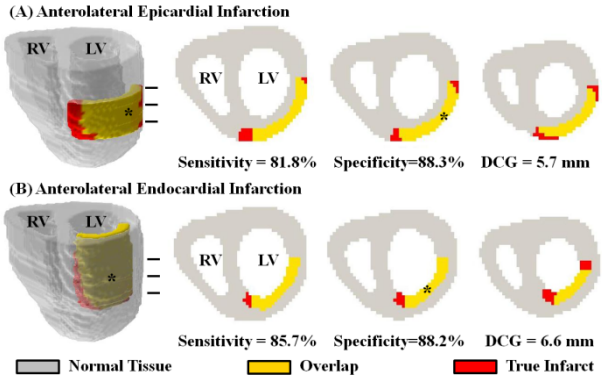

Figure 3. (A) Anterolateral epicardial infarct. (B) Anterolateral endocardial infarct. The black asterisks indicate the spatial-maximum ECD localized on epicardium/endocardium. The black lines represent the axial 2-D slices displayed on the right panel.

3.3. Effects of Noise Level, Electrode Number and Geometry Uncertainty

Figure 4(A) shows the averaged accuracy over 114 transmural infarcts with various noises (0, 5, 10, 15, 20, and 30μV). Apparently, a higher noise level leads to a slight decrease of sensitivity and specificity, and a minor increase of the DCG. The overall performance of the proposed approach is robust against noise: even with 30-μV additive noise, the proposed method can still identify on average over 75.1% of the infarct with an averaged DCG of around 10 mm.

We also evaluated the effect of the electrode number by using various numbers of electrodes (256, 205, 182, 156, and 98). Figure 4(B) suggests while more electrodes generally provide better performance, reasonable results were still obtained with limited electrode number. With 98 electrodes, the performance is comparable to the situation with 205 electrodes, as supported by the similar sensitivities (81.8% vs. 83.4%), specificities (82.8% vs. 82.2%), and DCG (7.4 mm vs. 6.5 mm), respectively.

The effects of the volume conductor modeling errors were evaluated by including torso geometry uncertainty and heart position uncertainty. The heart position was shifted by 4 mm from left to right (error A) or from the front to back (error B), while the torso volume was either expanded (error C) or reduced (error D) by 10%. We also investigated the situation of combining 10% dilation of the torso geometry with 4mm rightward transition of the heart (error A&C). Fig. 4(C) shows that even with the existence of both geometric error and heart position shifting (error A&C), this method still obtained a reasonable sensitivity of 78.3%, a specificity of 80.8%, and DCG of 9.8 mm. Thus the proposed method possessed reasonable robustness against modeling errors.

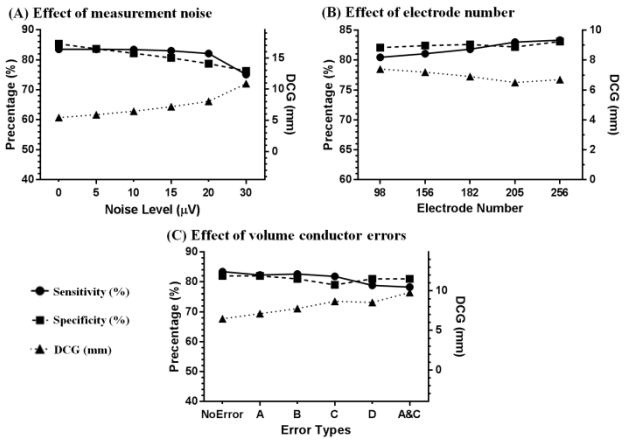

Figure 4. (A) effects of additive noises; (B) effects of numbers of electrodes; (C) effects of volume conductor modeling errors. 'No error': without volume conductor modeling error; 'A': heart shifting 4 mm from left to right; 'B': heart shifting 4 mm from front to back; 'C': torso expanded by 10%; 'D': torso reduced by 10%; 'A & C': combination of error A and C.

4. Discussion

In the present study, we have developed a new method for noninvasive imaging of the MI substrates based on physically modeling the cardiac electrical sources using the equivalent current density (ECD) distribution throughout the ventricular myocardium during the S-T segment. Comprehensive computer simulation studies were performed by simulating a large amount of transmural infarctions, epicardial infarctions and endocardial infarctions. The simulation results indicated that: 1) under 10μV GWN, the transmural infarction can be identified with an average sensitivity of 83.4%, specificity of 82.2%, and DCG of 6.5 mm over 114 cases, respectively; 2) the proposed method is able to provide information with respect to the substrate depth (epicardium vs. endocardium); 3) A reasonably good imaging performance can still be obtained under higher noise level, fewer BSPM electrodes, and mild volume conductor modeling errors, respectively.

5. Conclusions

In conclusion, we have proposed a novel method for noninvasive imaging of the myocardial infarction substrate throughout the 3D myocardium using the equivalent current density model. The comprehensive computer simulation results suggest that the proposed method is feasible to non-invasively estimate transmural and surface infarction, and to provide information with respect to epicardial infarction and endocardial infarction.

Acknowledgements

This work was supported in part by NIH RO1HL080093 and NSF CBET-0756331.

References

[1] Lazzara R, El-Sherif N, Hope RR, Scherlag B. Ventricular arrhythmias and electrophysiological consequences of myocardial ischemia and infarction. Circ Res 1978; 42:740-749.

[2] Oster HS, Taccardi B, Lux RL, Ershler PR, Rudy Y. Noninvasive electrocardiographic imaging: reconstruction of epicardial potentials, electrograms, and isochrones and localization of single and multiple electrocardiac events. Circulation 1997; 96:1012-1024.

[3] Cuppen JJM, Van Oosterom A. Model Studies with the Inversely Calculated lsochrones of Ventricular Depolarization. IEEE Trans Biomed Eng 1984; BME-31:652-659.

[4] Li G, He B. Localization of the site of origin of cardiac activation by means of a heart-model-based electrocardiographic imaging approach. IEEE Trans Biomed Eng 2001;8:660-669.

[5] He B, Li G, Zhang X. Noninvasive three-dimensional activation time imaging of ventricular excitation by means of a heart-excitation-model. Phys. Med. Biol. 2002;47:4063-4078.

[6] Liu Z, Liu C, He B. Noninvasive reconstruction of three-dimensional ventricular activation sequence from the inverse solution of distributed equivalent current density. IEEE Trans Med Imaging 2006;25:1307-18.

[7] Han C, Pogwizd S, Killingsworth C, Zhou Z, He B. Noninvasive cardiac activation imaging of ventricular arrhythmias during drug-induced QT prolongation in the rabbit heart. Heart Rhythm 2013;10:1509-1515.

[8] Miller W. Geselowitz DB. Simulation studies of the electrocardiogram. I. the normal heart. Circ Res 1978; 43:301-315.

[9] Wang JZ, Williamson SJ, Kaufman L. Magnetic source images determined by a lead-field analysis: The unique minimum-norm least-squares estimation. IEEE Trans Biomed Eng 1992;39:665-675.

[10] Pascual-Marqui RD, Skrandies W. Reply to comments by hamalainen, ilmoniemi and nunez. ISBET Newslett 1995;6:16–28.

[11] Hansen PC. Analysis of discrete ill-posed problems by means of the L-curve. SIAM Rev 1992;34:561-580.

[12] Cerqueira MD, Weissman NJ, Dilsizian V, Jacobs AK, Kaul S, Laskey WK, Pennell DJ, Rumberger JA, Ryan T, Verani MS. Standardized myocardial segmentation and nomenclature for tomographic imaging of the heart. Circulation 2002;105:539-542.

Address for correspondence.

Zhaoye Zhou.
7-105 Hasselmo Hall
312 Church St. SE
Minneapolis, MN 55455